Simulation of Diffusion Time of Small Molecules in Protein Crystals

Ways & Means

Silvano Geremia,[1,*] Mara Campagnolo,[1]
Nicola Demitri,[1] and Louise N. Johnson[2]
[1] Center of Excellence in Biocrystallography
Department of Chemical Sciences
University of Trieste
via L. Giorgieri 1
34127 Trieste
Italy
[2] Laboratory of Molecular Biophysics
Department of Biochemistry
University of Oxford
South Parks Road
OX1 3QU Oxford
United Kingdom

Summary

A simple model for evaluation of diffusion times of small molecule into protein crystals has been developed, which takes into account the physical and chemical properties both of protein crystal and the diffusing molecules. The model also includes consideration of binding and the binding affinity of a ligand to the protein. The model has been validated by simulation of experimental set-ups of several examples found in the literature. These experiments cover a wide range of situations: from small to relatively large diffusing molecules, crystals having low, medium, or high protein density, and different size. The reproduced experiments include ligand exchange in protein crystals by soaking techniques. Despite the simplifying assumptions of the model, theoretical and experimental data are in agreement with available data, with experimental diffusion times ranging from a few seconds to several hours. The method has been used successfully for planning intermediate cryotrapping experiments in maltodextrin phosphorylase crystals.

Introduction

Diffusion of ligands into preformed protein crystal is frequently used to study ligand binding and biological function in structural biology. The soaking technique is used for preparation of heavy-atom derivatives, cryoprotection of crystals, and the introduction of inhibitors, substrates, or effectors in crystal structures of enzymes. A crucial variable in the soaking experiments is the length of time required to achieve saturation from the solution of the diffusing molecule. The success of a diffraction experiment is often related to the soaking time. Long soaking times can result in crystal damage with loss of high-resolution data, while too short soaking times can result in the occupancy of the sites being too low to be detected. Despite the routine use of diffusion methods, there have been few results reported for the diffusion times of small molecules into protein crystals. Soaking times vary from a few seconds to days, and often there is no rational basis for the times used. A theoretical approach, by simulations of the diffusion process of small molecules into protein crystals, is important for planning and understanding soaking experiments.

The differential equations for the diffusion of small molecules into a protein crystal with binding and/or formation of reaction products are complex, and an analytic solution to the problem is possible only for some special cases (Crank, 1956). In the early years, calculations relating diffusion times to the rate of catalytic turnover were attempted in order to monitor conversion of substrate to product in the crystal. For example, for some particular steady-state conditions, equations have been derived for calculating a critical thickness of a plate protein crystal having the maximum enzymatic efficiency (Makinen and Fink, 1977; Sluyterman and de Graaf, 1969; Stoddard and Farber, 1995), but these equations are not readily extended for determining diffusion times, partly because of uncertainties in the modified diffusion coefficient (Bishop and Richards, 1968; Fink and Petsko, 1981; Sluyterman and de Graaf, 1969). In this paper, starting from Fick's first law, a generalized, simplified approach to the diffusion process is developed. The reliability of the simulation model has been validated on the basis of experimental data found in the literature. These experiments cover a wide range of situations: from small to relatively large diffusing molecules; crystals of different sizes and with low, high, or medium protein density; and with diffusion times from a few seconds to several hours.

The methods that have been used to measure diffusion of molecules into protein crystals have included X-ray diffraction (Alber et al., 1976; Johnson and Hajdu, 1990; Wyckoff et al., 1967a) (monitoring changes in X-ray intensities for some selected reflections as molecules are diffused into the crystal); birefringence of the crystal (James et al., 1980); spectroscopy (Bishop and Richards, 1968; O'Hara et al., 1995) (monitoring specific spectroscopic properties of molecules); fluorescence microscopy (Cvetkovic et al., 2004; Velev et al., 2000); and radioactivity counting of labeled molecules (Westbrook and Sigler, 1984). A summary of the different experimental approaches and the diffusion times of small molecules into protein crystals that have been reported in the literature is given in Table 1.

In these experiments, the diffusion time was measured under conditions in which there was low or no enzymatic activity. This was made possible in several ways: employing molecular species that having no specific interaction with enzymes (such as ammonium sulfate for ribonuclease-S and fluorescein for lysozyme); low-temperature conditions (such as for elastase); using mutant enzymes (such as the case of isocitrate dehydrogenase); or choosing inhibitor molecules of the enzymatic process. Among the experiments reported in Table 1, only six are described in sufficient detail to be chosen for the present study of simulation of the diffusion process in protein crystals. Further details of these

*Correspondence: geremia@units.it

Table 1. Experimental Diffusion Times for Molecules into Protein Crystals

Protein	Conditions of Experiment	Methods of Detection
Ribonuclease S (RnaseS) (Wyckoff et al., 1967a)	Change from 75% to 80% ammonium sulphate at room temperature. Replacement of bound iodo-uridine phosphate by 3 mM uridine phosphate at room temperature.	Monitoring changes in X-ray intensities.
β lactoglobulin (cross-linked crystals) (Bishop and Richards, 1968)	Diffusion of 0.02 M KBr. Diffusion of 0.02 M LiBr-uridylate. Diffusion of 5.7 mM BrPrOH.	X-ray fluorescence.
Glycogen phosphorylase b (GP) (Johnson and Hajdu, 1990)	Diffusion of 500 mM Phosphate, 100 mM Glucose-1-phosphate, 50 mM Maltoheptose, 100 mM Glucose, at room temperature.	Monitor of changes in X-ray intensities.
Elastase (Alber et al., 1976)	Diffusion of 3 mM N-carbobenzoyl-L-alanyl-p-nitrophenol into crystals and formation of the acyl intermediate at −55°C.	Monitor of changes in X-ray intensities.
Streptomyces griseus protease A (James et al., 1980)	Diffusion of 5 mM pentapeptide into crystal at room temperature.	Change in birefringence of the crystal.
Isocitrate dehydrogenase K230M (IDH) (O'Hara et al., 1995)	Diffusion of 200 mM isocitrate.	Changes in visible absorbance upon binding of substrate.
Δ^5–3–Ketosteroid isomerase (KIsom) (Westbrook and Sigler, 1984)	Diffusion of 4 mM radiolabeled progesterone in two hexagonal crystals. Diffusion of 25 mM nonradiolabeled competitive inhibitor 19-nortestosterone in two hexagonal crystals previously equilibrated with radiolabeled progesterone.	Radioactivity count of labeled substrate
Lysozyme (Cvetkovic et al., 2004)	Diffusion of fluorescein into tetragonal lysozyme crystals (T).	3D Laser scanning confocal microscopy visualization of the fluorescence signal.
Lysozyme (Velev et al., 2000)	Diffusion of pyrene derivatives into orthorombic lysozyme crystals (O).	Quantitative fluorescence microscopy.

experiments are given in the Supplemental Data available online.

Results and Discussion

A theoretical model was elaborated in order to reproduce the phenomenon of diffusion of small molecules in protein crystals. This model was validated with experimental values reported in the literature in a wide range of situations: from small diffusing molecules as sulfate and phosphate to larger molecules such as maltoheptaose; with crystals having very low protein density (70% solvent, as in IDH crystals), intermediate (40%–50% solvent, as in RnaseS and GP crystals), and very high (as in lysozyme crystals); with different crystal sizes; and with diffusion times from a few seconds to several hours. In Table 2, half saturation times obtained through simulations are compared with experimental values.

The simulations of diffusion in the GP crystals (Johnson and Hajdu, 1990) allow a test of the model with diffusing molecules of different sizes: from the small anion, dihydrogen phosphate (MW 97), to the larger molecule, maltoheptaose (MW 1153). Although the experimental measurements were conducted with relatively coarse time steps of 1.25 min (75 s), all simulations agree with the experimental data (Table 2). The half saturation times depend both on substrate dimensions, which influences the diffusion rate inside the crystal compartment, and the affinity constant, K_{eq}. Higher values of K_{eq}, reflecting weak binding, increase the saturation time. For GP, the effect of substrate dimensions is more important than enzyme affinity for substrates, and the theoretical results confirm this trend. For example, the small-molecule

phosphate binds with low affinity and diffuses in much faster than the larger molecule, maltoheptaose, which binds with relatively high affinity. In the diffusion experiment with glucose-1-phosphate into GP crystals, three reflections were monitored. Two of these gave consistent results for diffusion times, while the third appeared to be different. For the two reflections, the half saturation time corresponded to 1.30 min (78 s), which is very close to the 80 s obtained through theoretical evaluation.

Simulations of the IDH/isocitrate experiment are in agreement with the experimental data (O'Hara et al., 1995). This paper reports that about 10 s are necessary

Table 2. Comparison between the Half Equilibrium Time of Diffusion Process Obtained by Simulations and the Experimental Values

Protein/Diffusing Molecule	Calculated $t_{1/2}$	Experimental Value
GP/PO_4^{3-}	20 s	<1 min[a]
GP/Glc	25 s	~1 min[a]
GP/G1P	80 s	1.7 min[a] (120 s)
GP/G7	490 s	8 min[a] (480 s)
IDH/isocitrate	3.5 s	10 s[b]
RnaseS/NH4	120 s	90 s[a]
RnaseS/SO_4^{2-}	220 s	90 s[a]
RnaseS/U23P	15 hr[c]	12 h[a]
KetoIsom/progesterone	17 hr	2 days[b]
KetoIsom/nortestosterone	12 hr	<1 day[b]
Lysozyme T/fluorescein	16 min	~14 min
Lysozyme O/1-pyrsulphate	30 sec, 6.5 hr[d]	~6 hr

[a] Time evaluated for half saturation of enzyme sites.
[b] Time evaluated for complete saturation of enzyme sites.
[c] Time necessary for half substitution of 5-IU23P in the catalytic sites of RnaseS with U23P.
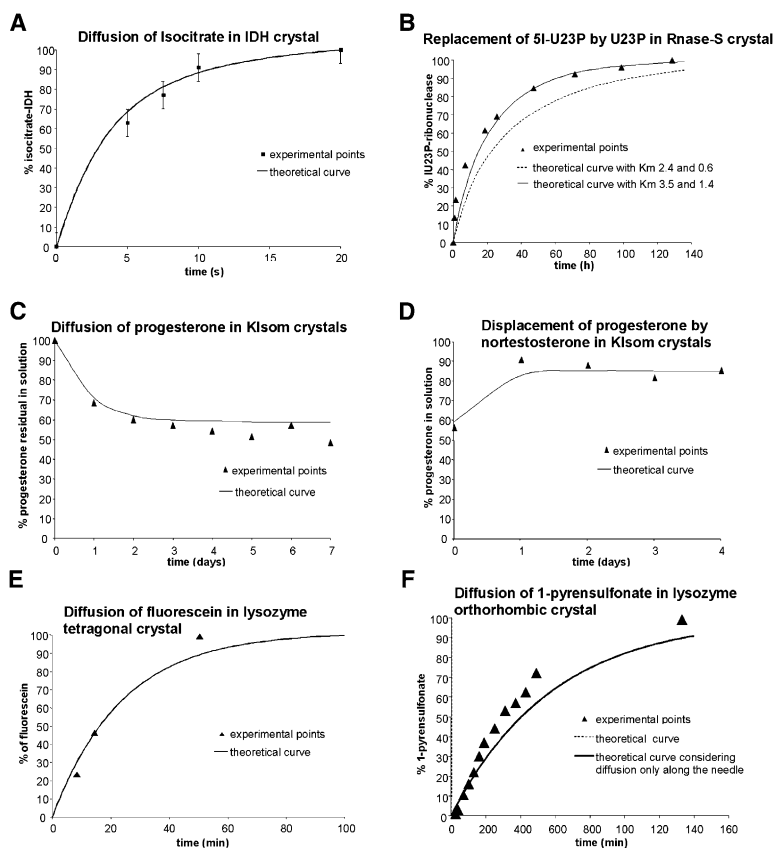[d] Considering diffusion only along the crystal channels.

Figure 1. Comparison between Experimental and Simulated Diffusion Times for Small Molecules into Protein Crystals

A good agreement is observed between calculated and experimental data, with experimental diffusion times ranging from a few seconds to days.

(A) Isocitrate diffusion into IDH crystals spectroscopically monitored by the reduction of NADP$^+$ to NADPH involved in the first step of the catalytic reaction. Experimental points are reported with an estimated experimental error of ±1 SEM.

(B) Replacement of the 5I-U23P in Rnase-S crystals with U23P monitored by X-ray diffraction. The experimental trend is well reproduced by the simulation with higher K_M values.

(C) Diffusion of progesterone in KIsom crystals monitored by radioactivity counting of labeled substrates. The simulation confirms that 2 days are sufficient to equilibrate the crystals with inhibitor solution.

(D) Progesterone is displaced out of the KIsom crystals in only 1 day when the nortesterone, a competitor with higher affinity, is added to the solution.

(E) Diffusion of fluorescein into lysozyme tetragonal crystals monitored by visualization of the fluorescence signal with 3D laser scanning confocal microscopy.

(F) Diffusion of 1-pyrensulphonate into lysozyme orthorhombic needle-shaped crystals monitored by quantitative fluorescence microscopy. The theoretical diffusion rate is calculated to be much faster (dotted curve) than the experimental value. The orthorhombic crystal structure is characterized by large pores (20 Å diameter) that coincide with the longest dimension of the crystal. If it is assumed that diffusion only occurs along these channels, the calculated diffusion rate (solid curve) is in agreement with the experimental data.

for the complete saturation of the catalytic sites of the IDH crystal mounted in a crystallographic flow cell and equilibrated with 200 mM isocitrate solution. In our calculation, a fixed concentration for the isocitrate in solution was set in order to simulate the flow cell conditions. We find that 3.5 s are sufficient to saturate half of the potential enzymatic sites, whereas after 10 s, about 90% of the crystal sites are populated by the substrate (Figure 1A).

The first simulated experiment with Ribonuclease S does not involve binding of substrates. The change in crystal diffraction is observed following the change of the ammonium sulfate concentration from 75% to 80% of saturation (4.8 M). Taking into account that the change in diffraction intensity can be related to the change in concentration of both ammonium and sulfate ions, the simulation was performed in order to evaluate the time necessary to reach 77.5% saturation for both ions in the crystal. The experimental value of 90 s is not far from the calculated values of 120 s for ammonium and 220 s for sulfate anions to diffuse into Rnase crystals with dimensions of 0.03 × 0.03 × 0.03 cm. The second simulated experiment involved the replacement of an inhibitor species in the Rnase crystal, 5-iodo-uridine 2'(3')-phosphate (5-IU23P), with an intermediate of enzyme catalysis, uridine 2'(3')-phosphate (U23P). Unfortunately, the K_M value, also necessary in the simulation to take into account the binding affinity, is known only for the natural substrate U23P. The literature reports two similar values of 2.4 and 3.5 mM for U23P and Rnase A pancreatic *Bos taurus* enzyme, respectively (Beintema et al., 1973). Wyckoff et al. (1967b), on the basis of difference Patterson maps, estimated the ratio of enzyme in the crystal bound to U23P with the enzyme bound to IU23P to be 0.67. From this value and the affinity constants for U23P, we estimated that the K_M for IU23P should be 0.6 mM (if K_M for U23P is 2.4 mM) or 1.4 mM (if K_M for U23P is 3.5 mM). The half saturation time, calculated for the diffusion of U23P in the absence of any inhibitors, corresponds to 8–9 hr. In two simulated cases employing crystals with dimensions of 0.04 × 0.06 × 0.06 cm, the time necessary for half replacement of 5-IU23P with U23P was determined to be 16 hr and 22 hr, depending on the K_M values chosen. The presence of the second competitive molecular species lowers the time required for the binding of U23P by more than a factor of two. The graph in Figure 1B reports the different curves simulating the diffusion process for the two different values of K_M. The curves describe the variation of percentage of IU23P bound in the enzyme crystal versus time. The points are extrapolated from the experimental curves in the work of Wyckoff et al. (1967a). The choice of the highest values of K_M (solid line) gives a prediction closer to the experimental measurements.

Calculations with crystals of Δ^5-3 ketosteroid isomerase enzyme were reproduced following the reported experimental procedure step by step (Westbrook and Sigler, 1984). Experimentally, a 5 μl aliquot of the mixture
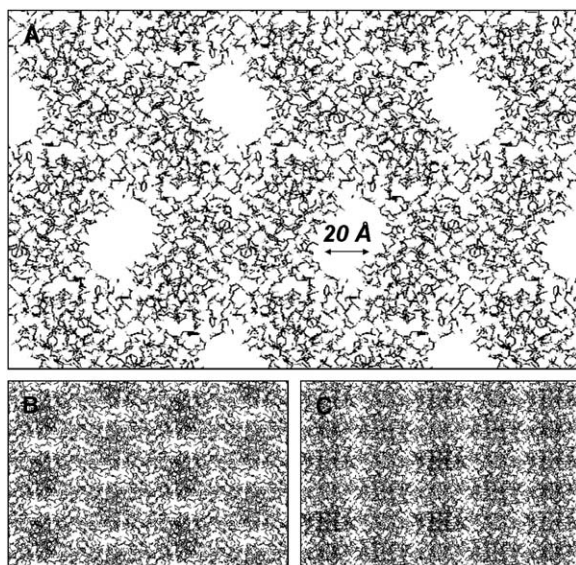
Figure 2. Views of the Crystal Packing along Cell Directions *a*, *b*, and *c* of the Orthorhombic Form of Lysozyme

The crystal packing reveals that the channels, which allow diffusion, are present only along the *a* cell axis.

Table 3. Parameters Used in the Simulation of the Diffusion Process: Crystal Dimensions and Geometrical Parameter $A/\Delta x$

Edges	*a* (cm)	*b* (cm)	*c* (cm)	A/Δx (cm)
RnaseS	0.03	0.03	0.03	0.36
RnaseS	0.04	0.06	0.06	0.68
GP	0.047	0.04	0.16	1.34
IDH	0.05	0.05	0.03	0.57
KIsom.	0.135	0.01	0.01	1.08
Lysozyme T	0.01	0.01	0.008	0.114
Lysozyme O	0.15	0.007	0.007	1.20

was taken every 24 hr to measure the progesterone concentration (see Supplemental Data). In our simulation, we considered both the variation of solution volume and presence of two protein crystals. The variation of progesterone concentration in solution was followed for 7 days before and 4 days after the addition of the competitive inhibitor 19-nortestosterone. The experimental and theoretical results are reported in Figures 1C and 1D. The points have been extrapolated from the experimental curve reported in Figure 2 of the article by Westbrook and Sigler (1984). When progesterone molecules diffuse into the crystals, the relative concentration in solution decreases (Figure 1C). When the higher-affinity competitor nortestosterone is added, it displaces the first inhibitor, whose concentration in solution, consequently, increases (Figure 1D). In the presence of crystals, the progesterone in solution approached the equilibrium in solution at 2.4 μM in 2 days, whereas in the second part of the experiment, the equilibrium was reached after only 24 hr, reaching 85% of its original value (4 μM). The theoretical curves reproduce both the rate by which the equilibrium is reached and the composition at equilibrium.

The interpretation of the diffusion of fluorescein molecules in tetragonal crystals of lysozyme is given in Figure 1E. Diffusing molecules do not interact specifically with the enzyme, so no affinity constant has been introduced in the process. The experimental points have been interpreted from spectra recorded by 3D laser scanning confocal microscopy, assuming that intensity is linear with concentration of fluorescein molecules inside the crystal (Cvetkovic et al., 2004). The final values are calculated from the average of the intensity profiles recorded along the three directions of diffusion orthogonal to the crystal surface. The first two points are very well predicted by the curve, and the third point is not far from the theoretical value. Experimentally, the saturated profile intensity was recorded after 50 min of diffusion. The simulation of the diffusion process shows that

after the same period the concentration of fluorescein molecules in the crystal is 90% of equilibrium.

The experiment with orthorhombic crystals of lysozyme is not well reproduced by our diffusion model. The dimensions of diffusing molecules of 1-pyrene sulfonate and the diffusion coefficient are similar to those of fluorescein. According to the theoretical curve, saturation of the crystal should take place in 2.5 min. Experimentally, diffusion is very slow; in fact, half time saturation is estimated to be about 6 hr (Figure 1F). The lysozyme orthorhombic crystals have a needle shape. Analysis of the crystal packing reveals an open pore structure with the presence of channels only along the "a" axis of the unit cell (Figure 2). If we consider the diffusion only along these channels, the calculated diffusion rate (solid curve in Figure 1F) follows the trend of the experimental dataset.

Conclusions

Starting from Fick's first law, a simplified approach to the diffusion of small molecules into protein crystals has been proposed. The kinetic constants used in the diffusion simulation model are calculated from the coordinates of the protein crystal structure and of the diffusing ligand and the crystal dimensions. The reliability of the simulation model has been validated on the basis of experimental data found in the literature. The simulation of diffusion revealed that the period of soaking necessary to saturate protein crystals is dependent on ligand dimensions, crystal shape, accessible volume, and binding affinity. For example, while a few seconds are sufficient to saturate a GPb crystal with phosphate, several days of soaking are necessary to equilibrate progesterone with KIsom crystals.

Simulations of the diffusion process of small molecules inside protein crystals are particularly important for planning and for understanding the soaking experiments of protein crystals in ligand solutions. Recently, we reported the X-ray studies on enzymatic catalysis in crystals of *Escherichia coli* maltodextrin phosphorylase (MalP) (Geremia et al., 2002). The catalytic event in crystals can be induced starting from binary complexes and employing soaking techniques to introduce the second substrate to form the reactive ternary complex. MalP catalysis can be followed either in the direction of oligosaccharide synthesis, using G1P plus oligosaccharide, or in the direction of phosphorylysis, using inorganic phosphate and oligosaccharide. We have shown that soaking crystals of MalP/G1P binary complex in oligosaccharide solution (maltopentose, G5; or maltotetraose, G4) triggered the enzymatic reaction in the direction of synthesis. The products of the catalytic events were trapped by cryocooling the crystals with a nitrogen

Table 4. Parameters Used in the Simulation of the Diffusion Process: Diffusion Coefficients, D, Calculated for the Diffusing Molecules

	D (HYDRO) (cm^2/s)	Correction Factor (6/n)	D (Corrected) (cm^2/s)	Handbook of Chemistry & Physics (cm^2/s)
Phosphate	9.2 E–06	1.33	1.2 E–05	8.79 E–06
Glucose	6.3 E–06	1.10	6.9 E–06	6.70 E–06
Glucose-1-P	5.6 E–06	1.05	5.9 E–06	
Heptaglucose	2.3 E–06	1.00	2.3 E–06	2.5 E–06[a]
Isocitrate	6.4 E–06	1.13	7.2 E–06	
Ammonium	1.2 E–05	1.80	2.2 E–05	1.96 E–05
Sulphate	1.0 E–05	1.42	1.4 E–05	1.33 E–05
Uridine 2′(3′)-P	5.4 E–06	1.05	5.6 E–06	
5I-Uridine 2′(3′)-P	5.1 E–06	1.03	5.3 E–06	
Progesterone	4.8 E–06	1.00	4.8 E–06	
19-Nortestosterone	5.0 E–06	1.03	5.1 E–06	
Fluorescein	5.1 E–06	1.03	5.2 E–06	4.8–5.5 E–06[b]
1-Pyrenesulfonic acid	5.4 E–06	1.05	5.7 E–06	

D values are corrected by the correction factor, n, of the Stokes-Einstein equation and compared with experimental values.
[a] Johnson and Hajdu, 1990.
[b] deBeer et al., 1997.

stream at 100K. The X-ray structures showed that in 20 min of soaking, the relatively large oligosaccharide substrates can diffuse into the crystals and that the enzymatic reaction had occurred with elongation of the oligosaccharide chain, disappearance of G1P, and formation of phosphate. For MalP and GP (the catalytic site of the bacterial MalP is almost identical to that found in the mammalian GP isoenzyme [Watson et al., 1999]), the rate-limiting step in the reaction is the interconversion of the ternary enzyme complex. In our experiments, we wished to trap the reaction intermediate. In order to do this, the soaking interval is most important, as the diffusion process of substrates into the crystal should be less than the rate-limiting step. Diffusion simulations that reproduced the experimental soaking conditions showed that the times for half saturation of the catalytic sites in MalP crystals for G5 and G4 substrates are 1.5 and 1 min, respectively. These calculations show that a long soaking time (more than 10 min) is needed for the saturation of the MalP enzyme with the oligosaccharide substrate, and is too slow for time-resolved experiments. On the other hand, simulation of diffusion times for phosphate ions into MalP/G5 crystals showed that the time for half saturation of the crystal was less than 2 s. These data suggested that it might be possible to study MalP enzymatic catalysis in the crystal in the direction of phosphorolysis using very short times for soaking. The electron density maps of the complex, obtained through the soaking of MalP/G5 crystal in phosphate solution (20 s), showed the presence an oxocarbonium ion in the catalytic channel (unpublished results). The oxocarbonium ion was postulated to be the transition state of the unusual internal nucleophilic substitution (S_Ni) proposed for the phosphorylase catalytic mechanism (Klein et al., 1986). This experimental result represents the first structural characterization of the long-lived oxocarbonium ion, and provides direct support for the existence of this intermediate. In this respect, the simplified diffusion model reported in this paper was a key factor in the design of these experiments.

Finally, it should be noted that in reproducing the diffusion experiments, we did not consider catalysis in the crystal (i.e., the analysis was restricted to binding events). However, using this approach it is possible to make time-course simulations with or without steady-state conditions, introducing reaction kinetics, binding and dissociation equilibria, formation of intermediates, etc., and the diffusion of several ligands, substrates, or products.

Experimental Procedures

A simple model for evaluation of diffusion times of small molecule into protein crystals was developed, which takes into account the physical and chemical properties both of the protein crystal and the diffusing molecules. The model also includes consideration of binding and the affinity of binding of a ligand to the protein.

Table 5. Parameters Used in the Simulation of the Diffusion Process: Kinetic Constants of Diffusion, k_D', Corrected by the Fraction of the Accessible Volume Dependent on the Dimension—Stokes Radius—of the Diffusing Molecules

Protein and Substrate	PDB Code	Stokes R (cm)	Accessible Volume, Φ (%)	k_D' (cm^3/s)
GP/PO4	1HCU	2.3 E–08	29	1.4 E–06
GP/Glc		3.4 E–08	26	6.4 E–07
GP/G1P		3.8 E–08	26	5.4 E–07
GP/G7		9.4 E–08	13	5.5 E–08
IDH/isocitrate	1IDC	3.3 E–08	59	1.4 E–06
Rnase S/NH4	1Z3L	1.8 E–08	14	1.6 E–07
Rnase S/SO4		2.1 E–08	13	8.5 E–08
Rnase S/U23P		4.0 E–08	9.5	3.5 E–08
Rnase S/I-U23P		4.2 E–0.8	9.0	2.9 E–08
KIsom/progesterone	8CHO	4.4 E–0.8	32	5.3 E–07
KIsom/nortestosterone		4.2 E–0.8	33	5.8 E–07
Lysozyme/fluorescein	1HEL	4.2 E–0.8	3.1	5.7 E–10
Lysozyme/1-pyrenesulfonic	1HSW	4.0 E–0.8	17	1.9 E–07

Table 6. Parameters Used in the Simulation of the Diffusion Process: Equilibrium Constant, K_{eq}, for the EL_c Complex Dissociation

	$[L_s]$ (mM)	$[E]$ (mM)	Crystal Volume (cm^3)	K_{eq} (mM)
GP/PO4	500	6.9	3.0 E–04	40[a]
GP/Glc	100	6.9	3.0 E–04	1.7[b]
GP/G1P	100	6.9	3.0 E–04	10[c]
GP/G7	50	6.9	3.0 E–04	1[c]
IDH/isocitrate	200	8	1.0 E–04	6[d]
RnaseS/NH4	7680	60	2.7 E–05	
RnaseS/SO4	3840	60	2.7 E–05	
Rnase S/U23P	3	[ELc] 19.2	14.4 E–05	3.5[e]
Rnase S/I-U23P	0	[ELc] 40.8	14.4 E–05	1.4[f]
KetoIsom/progesterone	0.004	42	2 × 1.4 E–05	6.4 E–03[g]
KetoIsom/nortestosterone	0.025	42	2 × 1.4 E–05	5.2 E–03[g]
Lysozyme T/fluorescein	0.08	56	8 E–07	
Lysozyme O/1-pyrsulphate	1	57	7.35 E–06	

Values are employed to estimate the strength of binding interactions between enzymes and the proper substrate or inhibitor molecules during diffusion simulation. $[L_s]$ = concentration of substrate in the solution compartment; $[E]$ = crystal enzyme concentration; $[EL_c]$ = concentration of the complex in the protein crystal.
[a] Hajdu et al., 1987.
[b] Johnson, 1992.
[c] Johnson and Hajdu, 1990.
[d] Lee et al., 1995.
[e] Beintema et al., 1973.
[f] See text.
[g] Batzold et al., 1976.

Simulations are compared with the available experimental values that are summarized in Table 1 and the Supplemental Data.

The Model for the Diffusion Process in Crystal
The diffusion rate of small particles is described by Fick's first law:

$$J = -D\frac{dC}{dx}, \tag{1}$$

where J is the flux of particles through unity area, D is the diffusion coefficient, and dC/dx is the variation of concentration with the distance x. The negative sign indicates that particles are moving toward decreasing gradient of concentration. J has the dimension of a velocity per unit area [mol s^{-1} cm^{-2}], and the diffusion coefficient D is expressed in units of cm^2 s^{-1}. The same equation expressed in discrete terms and multiplied by a given surface area, A, gives the total flux of particles through A:

$$JA = -DA\frac{\Delta C}{\Delta x}. \tag{2}$$

The product JA describes the mean molecular diffusion, v (mol s^{-1}), per path length, Δx. If the geometric properties of the system are constant, v is proportional to concentration gradient ΔC by a factor k_D, which expresses the diffusion kinetic constant:

$$k_D = D\frac{A}{\Delta x} \tag{3}$$

$$v = -k_D\Delta C. \tag{4}$$

Simulations of the diffusion process were performed by the program GEPASI (Mendes, 1993). This program permits the treatment of a system with multiple compartments. In order to simulate the diffusion process, two compartments have been defined: solution and crystal. The enzyme is confined in the crystal compartment, while substrates, products, or ligands are in both compartments. The diffusion event of ligands during a soaking experiment may be expressed as an equilibrium process between molecules diffusing from solution to crystal and vice versa. The diffusion process between the two compartments has been considered as a "reaction" of type $[L_S] \rightleftarrows [L_C]$ (where $[L_S]$ and $[L_C]$ indicate ligand concentration present in solution and in crystal, respectively), with reversible mass action kinetics having $v = (k_1)[L_S] - (k_{-1})[L_C]$ where v (mol s^{-1}) is the total net flux of ligand L from the solution L_S to the crystal L_C or vice versa, and k_1 and k_{-1} have dimensions in $cm^3 s^{-1}$. At equilibrium, the concentration of L inside and outside the crystal should be the same and the net flux equal to zero; as a consequence, $(k_1) = (k_{-1})$.

Flux rate has been described using Equation 4, where ΔC is substituted by ΔL ($\Delta L = [L_S] - [L_C]$) and k_D is the diffusion kinetic constant.

$$v = -k_D\Delta L \tag{5}$$

This implies that the total net flux of particles is proportional to the difference of the L concentration in the two compartments. Equation 5 may be applied if $k_D = DA/\Delta x$ is known. To evaluate the diffusion constant, we approximate the crystal as a parallelepiped with edges a, b, c and the total flux of material as the sum of the flux thought the 6 crystal faces. For each ab face, the mean $A/\Delta x$ is $ab/(c/2)$ and, considering all crystal surfaces, the geometrical parameter is $A/\Delta x = 4(ab/c + bc/a + ac/b)$. This geometrical parameter calculated for the crystals used in simulations is reported in Table 3.

Not all the diffusion coefficients D of the molecules involved in the test experiments are available in the literature. The diffusion coefficients in water at 20ºC of the molecules involved in these experiments were evaluated using the program HYDRO (a program developed for macromolecules) (Garcia de la Torre et al., 1994) starting from rigid molecular models of the substrates. The diffusion coefficients have been calculated starting from the 3D model of the molecules and using the van der Waals radii of the atoms without considering the hydration sphere, since it has been shown that small molecules diffuse more rapidly than predicted by the Stokes-Einstein equation, and their behavior is similar to molecules not wetted by the solvent (Edward, 1970). Stokes-Einstein equation ($D = kT/6\pi\eta r$), where k is Boltzmann's constant and T the absolute temperature, predicts the diffusion coefficient for spherical molecules of Stokes radius r moving with uniform velocity in a continuous fluid of viscosity η. However, it has been observed that the diffusion coefficient, calculated with this formula and using the van der Waals radius of the molecule, is underestimated for small molecules with radii below 5 Å. Edwards (Edward, 1970) used an empirical correction factor $6/n$ to the constant 6 of the Stokes equation in order to take into account this discrepancy. The dependence of the numerical factor $6/n$ (which is 1 for molecules with radii > 5 Å) of the Stokes-Einstein equation on the molecular radii has been evaluated using 44 small molecules of known diffusion in water. The correction factors $6/n$ for the small molecules analyzed in this paper have been extrapolated from the experimental curve reported by Edwards.

The diffusion coefficients calculated by the HYDRO program have been adjusted by these correction factors (Table 4). The diffusion

coefficients calculated in this way are in good agreement with the experimental values reported in the Handbook of Chemistry and Physics (Chemical Rubber Company, 1995) as shown in Table 4.

A further correction applied to Equation 5 is the factor Φ that takes into account the accessible volume to substrate in the total volume of crystal. In a theoretical paper (Tomadakis and Sotirchos, 1993) on simulation of random walking molecules in cells with randomly distributed cylinders, it is shown that the effective transport coefficient, D, of the walking molecule should be corrected for the square of the accessible volume, Φ (Figure 3 in the article by Tomadakis and Sotirchos (1993). In the crystals taken as examples, the fractions of the accessible volume have been evaluated from the coordinate files (PDB entries are specified in Table 5) omitting substrates and solvent molecules. Then, using CCP4 programs (CCP4, 1994) (in order SFALL, MAPMASK, and NCSMASK), a mask was calculated for each protein in the asymmetric unit, considering a mean van der Waals radius of 1.7 Å. The starting mask was expanded by a volume (2.8 Å radius) corresponding to a first hydrated shell. Through expansion and successive contraction of the mask by a radius equal to the Stokes radius of the diffusing molecule, the volume not accessible to the molecule has been removed. The introduction into the model of a monolayer of water molecules covering the protein surface reduces the accessible volume for molecules, lowering the diffusion process. This approximation, which fixes a shell of water molecules around the protein surface, simulates multiple effects of the interactions between protein and solvent and diffusing molecules that are difficult to evaluate quantitatively (Malek et al., 2004).

The constant k_D' reported in Table 5 was calculated according to the equation:

$$k_D' = \left(D \frac{A}{\Delta x} \right) \Phi^2. \tag{6}$$

A local program called KD-CALC, linked with the HYDRO and CCP4 packages, has been developed in order to calculate the kinetic constants of diffusion starting from the crystal dimensions and PDB files of the protein crystal structure and of the diffusing molecule.

The starting conditions for the simulation processes with GEPASI are reported in Table 6. In some simulations, GP, IDH, Rnase, and Ketolsom, the equilibrium of dissociation of the protein-small molecule complex ($EL_c = E + L_c$) has been introduced in the crystal compartment. The K_{eq} constant has been approximated with the Michaelis-Menten constant, K_M, when diffusing molecules were substrates, or with the inhibition constant, K_I, when molecules were inhibitors of the enzyme.

Programs for kinetic constants calculations and files for GEPASE simulations are available online at http://www.units.it/~ceb/diffusion/.

Supplemental Data

Supplemental Data, including additional Experimental Procedures used in this work, are available online at http://www.structure.org/cgi/content/full/14/3/393/DC1/.

Acknowledgments

References

Alber, T., Petsko, G.A., and Tsernoglou, D. (1976). Crystal structure of elastase-substrate complex at −55 degrees C. Nature *263*, 297–300.

Batzold, F.H., Benson, A.M., Covey, D.F., Robinson, C.H., and Talalay, P. (1976). The delta 5–3-ketosteroid isomerase reaction: catalytic mechanism, specificity and inhibition. Adv. Enzyme Regul. *14*, 243–267.

Beintema, J.J., Campagne, R.N., and Gruber, M. (1973). Rat pancreatic ribonuclease: I. Isolation and properties. Biochim. Biophys. Acta *310*, 148–160.

Bishop, W.H., and Richards, F.M. (1968). Properties of liquids in small pores: rates of diffusion of some solutes in cross-linked crystals of beta-lactoglobulin. J. Mol. Biol. *38*, 315–328.

CCP4 (Collaborative Computational Project, Number 4) (1994). The CCP4 suite: programs for protein crystallography. Acta Crystallogr. D Biol. Crystallogr. *50*, 760–763.

Chemical Rubber Company (1995). CRC Handbook of Chemistry and Physics, 83rd Edition (Cleveland, OH: CRC Press).

Crank, J. (1956). The Mathematics of Diffusion. (Oxford, UK: Oxford University Press).

Cvetkovic, A., Straathof, A.J., Hanlon, D.N., van der Zwaag, S., Krishna, R., and van der Wielen, L.A. (2004). Quantifying anisotropic solute transport in protein crystals using 3-D laser scanning confocal microscopy visualization. Biotechnol. Bioeng. *86*, 389–398.

deBeer, D., Stoodley, P., and Lewandowski, Z. (1997). Measurement of local diffusion coefficients in biofilms by microinjection and confocal microscopy. Biotechnol. Bioeng. *53*, 151–158.

Edward, J.T. (1970). Molecular volumes and the Stokes-Einstein equation. J. Chem. Educ. *47*, 261–270.

Fink, A.L., and Petsko, G.A. (1981). X-ray cryoenzymology. Adv. Enzymol. Relat. Areas Mol. Biol. *52*, 177–246.

Garcia de la Torre, J., Navarro, S., Lopez Martinez, M.C., Diaz, F.G., and Lopez Cascales, J.J. (1994). HYDRO: a computer program for the prediction of hydrodynamic properties of macromolecules. Biophys. J. *67*, 530–531.

Geremia, S., Campagnolo, M., Schinzel, R., and Johnson, L.N. (2002). Enzymatic catalysis in crystals of *Escherichia coli* maltodextrin phosphorylase. J. Mol. Biol. *322*, 413–423.

Hajdu, J., Acharya, K.R., Stuart, D.I., McLaughlin, P.J., Barford, D., Oikonomakos, N.G., Klein, H., and Johnson, L.N. (1987). Catalysis in the crystal: synchrotron radiation studies with glycogen phosphorylase b. EMBO J. *6*, 539–546.

James, M.N., Sielecki, A.R., Brayer, G.D., Delbaere, L.T., and Bauer, C.A. (1980). Structures of product and inhibitor complexes of *Streptomyces griseus* protease A at 1.8 A resolution: a model for serine protease catalysis. J. Mol. Biol. *144*, 43–88.

Johnson, L.N. (1992). Glycogen phosphorylase: control by phosphorylation and allosteric effectors. FASEB J. *6*, 2274–2282.

Johnson, L.N., and Hajdu, J. (1990). Synchrotron studies on enzyme catalysis in crystals. In Synchrotron Radiation in Biophysics, S. Hasnian, ed. (Chichester, UK: Ellis Horwood Ltd.), pp. 142–155.

Klein, H.W., Im, M.J., and Palm, D. (1986). Mechanism of the phosphorylase reaction: utilization of D-gluco-hept-1-enitol in the absence of primer. Eur. J. Biochem. *157*, 107–114.

Lee, M.E., Dyer, D.H., Klein, O.D., Bolduc, J.M., Stoddard, B.L., and Koshland, D.E., Jr. (1995). Mutational analysis of the catalytic residues lysine 230 and tyrosine 160 in the NADP(+)-dependent isocitrate dehydrogenase from *Escherichia coli*. Biochemistry *34*, 378–384.

Makinen, M.W., and Fink, A.L. (1977). Reactivity and cryoenzymology of enzymes in the crystalline state. Annu. Rev. Biophys. Bioeng. *6*, 301–343.

Malek, K., Odijk, T., and Coppens, M.O. (2004). Diffusion in protein crystals: a computer simulation. Chemphyschem *5*, 1596–1599.

Mendes, P. (1993). GEPASI: a software package for modelling the dynamics, steady states and control of biochemical and other systems. Comput. Appl. Biosci. *9*, 563–571.

O'Hara, P., Goodwin, P., and Stoddard, B. (1995). Direct measurement of diffusion rates in enzyme crystals by video absorbance spectroscopy. J. Appl. Crystallogr. *28*, 829–834.

Sluyterman, L.A., and de Graaf, M.J. (1969). The activity of papain in the crystalline state. Biochim. Biophys. Acta *171*, 277–287.

Stoddard, B.L., and Farber, G.K. (1995). Direct measurement of reactivity in the protein crystal by steady-state kinetic studies. Structure *3*, 991–996.

Tomadakis, M., and Sotirchos, S. (1993). Transport properties of random arrays of freely overlapping cylinders with various orientation distributions. J. Chem. Phys. *98*, 616–626.

Velev, O.D., Kaler, E.W., and Lenhoff, A.M. (2000). Surfactant diffusion into lysozyme crystal matrices investigated by quantitative fluorescence microscopy. J. Phys. Chem. B *104*, 9267–9275.

Watson, K.A., McCleverty, C., Geremia, S., Cottaz, S., Driguez, H., and Johnson, L.N. (1999). Phosphorylase recognition and phosphorolysis of its oligosaccharide substrate: answers to a long outstanding question. EMBO J. *18*, 4619–4632.

Westbrook, E.M., and Sigler, P.B. (1984). Enzymatic function in crystals of delta 5–3-ketosteroid isomerase: catalytic activity and binding of competitive inhibitors. J. Biol. Chem. *259*, 9090–9095.

Wyckoff, H.W., Doscher, M., Tsernoglou, D., Inagami, T., Johnson, L.N., Hardman, K.D., Allewell, N.M., Kelly, D.M., and Richards, F.M. (1967a). Design of a diffractometer and flow cell system for X-ray analysis of crystalline proteins with applications to the crystal chemistry of ribonuclease-S. J. Mol. Biol. *27*, 563–578.

Wyckoff, H.W., Hardman, K.D., Allewell, N.M., Inagami, T., Tsernoglou, D., Johnson, L.N., and Richards, F.M. (1967b). The structure of ribonuclease-S at 6 A resolution. J. Biol. Chem. *242*, 3749–3753.